Available online at www.sciencedirect.com
SCIENCE DIRECT
Journal of Organometallic Chemistry 691 (2006) 765–778
Journal of Organometallic Chemistry
www.elsevier.com/locate/jorganchem

Liquid crystal behaviour of ionic allylpalladium complexes containing 2-pyrazolylpyridine as bidentate *N*,*N*′-ligand

M.C. Torralba [a], M. Cano [a,*], J.A. Campo [a], J.V. Heras [a], E. Pinilla [a,b], M.R. Torres [b]

[a] *Departamento de Química Inorgánica I, Facultad de Ciencias Químicas, Universidad Complutense, E-28040 Madrid, Spain*
[b] *Laboratorio de Difracción de Rayos-X, Facultad de Ciencias Químicas, Universidad Complutense, E-28040 Madrid, Spain*

Received 18 July 2005; received in revised form 26 September 2005; accepted 26 September 2005
Available online 23 November 2005

Abstract

Two types of Pd-complexes containing the new *N*,*N*′-ligands 2-[3-(4-alkyloxyphenyl)pyrazol-1-yl]pyridine (pz^Rpy; R = $C_6H_4OC_nH_{2n+1}$, *n* = 6 (hp), 10 (dp), 12 (ddp), 14 (tdp), 16 (hdp), 18 (odp)) (**1**–**6**), namely *c*-[$Pd(Cl)_2(pz^Rpy)$] (**7**–**10**) and *c*-[$Pd(\eta^3\text{-}C_3H_5)(pz^Rpy)]BF_4$ (**11**–**16**), have been synthesised and characterised by different spectroscopic techniques. Those members of the second type containing the largest chains (R = ddp **13**, tdp **14**, hdp **15**, odp **16**) have been found to have liquid crystal properties showing smectic A mesophases. By contrast, neither the free ligands pz^Rpy nor their related *c*-[$Pd(Cl)_2(pz^Rpy)$] complexes exhibited mesomorphism. The new synthesised metallomesogens are mononuclear complexes with an unsymmetrical molecular shape as deduced from the X-ray structures of *c*-[$Pd(\eta^3\text{-}C_3H_5)(pz^Rpy)]BF_4$ (R = hp, **11**; dp, **12**). Both compounds, which are isostructural, show a distorted square-planar environment on the palladium centres defined by the allyl and the bidentate pz^Rpy ligands. The crystal structure reveals that both the counteranion and the pz^Rpy ligand function as a source of hydrogen-bonding and intermolecular π···π contacts resulting in a ^2D supramolecular assembly.

Keywords: Long-chained pyrazolylpyridine ligands; Palladium(II) complexes; Mesomorphism

1. Introduction

We are currently concerned with the design and synthesis of metallomesogens based on pyrazole or related ligands containing long-chained substituents.

In a previous work, we reported the liquid crystal behaviour of *t*-[$Pd(Cl)_2(Hpz^R)_2$] (**a**) complexes (Hpz^R = 3-alkyloxysubstituted pyrazole; R = $C_6H_4OC_nH_{2n+1}$) which exhibited a conventional rod-like molecular geometry concerning with the *trans* orientation of the pyrazol groups [1]. By contrast, the free Hpz^R ligands resulted to have no mesomorphic properties [1,2], this feature being associated with their short molecular lengths which were about half the complexes **a** [1].

Related with these results we were also involved in investigating the liquid crystal behaviour of the compounds *c*-[$Pd(Cl)_2(pz^{R2}py)$] (**b**), where $pz^{R2}py$ were the unsymmetrical bidentate ligands 2-[3,5-bis(4-alkyloxyphenyl)pyrazol-1-yl]pyridine [3]. These complexes exhibited mesomorphism, which was not extensively different to that of *t*-[$Pd(Cl)_2(Hpz^R)_2$] [1]. In both types of compounds, **a** and **b**, the mesophases presented an analogous accessibility, but the latter exhibiting higher stability. The above results allowed us to consider that the molecular shape and lowering the symmetry of complexes by introducing pyrazolylpyridine-type ligands were a successful strategy on metallomesogenic compounds.

On the other hand the relationship between chemical structure and mesomorphism has been extensively investigated in the field of liquid crystals. In particular, deviations from the rod-like molecular shape or a non-adequate

* Corresponding author. Fax: +34 91 3944352.
E-mail address: mmcano@quim.ucm.es (M. Cano).

0022-328X/$ - see front matter © 2005 Elsevier B.V. All rights reserved.
doi:10.1016/j.jorganchem.2005.09.053

molecular length-to-width ratio have been proved to prevent the mesomorphism of proposed molecules as calamitic materials [1,3–5].

Following these precedents we are now interested in the study of a new type of bidentate pyrazolylpyridine ligands (pz^Rpy) containing only one alkyloxyphenyl ($C_6H_4OC_nH_{2n+1}$) substituent chain at the 3-position of the pyrazolyl group, as well as their complexes with $PdCl_2$ and $[Pd(\eta^3\text{-}C_3H_5)]^+$ fragments. We propose that, by coordination of the pz^Rpy ligands to the $PdCl_2$ fragment, the molecular length should be reduced about half the related liquid-crystal compounds *c*-$[Pd(Cl)_2(pz^{R2}py)]$ [3], this fact being useful to evaluate their influence on the mesomorphic properties. As extension we also try to consider the effectivity of $[Pd(\eta^3\text{-}C_3H_5)]^+$ as metallic fragment towards the same pz^Rpy ligands in order to get new cationic complexes of the type *c*-$[Pd(\eta^3\text{-}C_3H_5)(pz^Rpy)]^+$ as potential liquid crystals.

Mesomorphism of palladium complexes containing bidentate ligands has been specially developed on neutral cyclopalladated $N(sp^2)$-Pd-$C(sp^2)$ species. In this context, azobenzene, benzylideneanilines, imines or substituted bipyridine ligands, among others, gave rise to neutral mono- or dinuclear cyclopalladated complexes, most of them showing low transition temperatures and high thermal stability [6–12]. Several *N*,*N*-coordinated bipyridine-type ligands have been also proved to induce mesomorphism on $PdCl_2$ complexes [13].

In contrast, ionic metallomesogens are a more restricted area inside the molecular and supramolecular species [14], and from the best of our knowledge only two examples containing palladium have been described [15,16]. In particular, an ionic *ortho*-metallated complex $[Pd(L)(bpy)]^+$ containing the mesogenic 5-(1-hexyl)-2-{[4′-(1-undecyloxy)phenyl]}pyrimidine (HL) and 2,2′-bipyridine as coligand was proved to have mesomorphism when it was isolated as BF_4^- salt, but larger anions as PF_6^- or SbF_6^- suppressed the liquid crystal behaviour, this behaviour reflecting the influence of uncoordinated counterion [15].

In the present work, we describe the preparation, characterisation and study of a family of new 2-[3-(4-alkyloxyphenyl)pyrazol-1-yl]pyridine ligands (pz^Rpy; $R = C_6H_4OC_nH_{2n+1}$, $n = 6$ (hp), 10 (dp), 12 (ddp), 14 (tdp), 16 (hdp), 18 (odp)) (**1**–**6**) and their complexes with $PdCl_2$ and $[Pd(\eta^3\text{-}C_3H_5)]^+$ groups (Scheme 1). Both free ligands and their dichloropalladium derivatives have not shown liquid crystal behaviour. By contrast, the related allylpalladium complexes with BF_4^- as counteranion exhibit mesomorphic properties.

As extension two new related derivatives containing the same cationic metal complex and different counteranions (PF_6^-, $CF_3SO_3^-$) have also been studied and proved to have liquid crystal behaviour.

The palladium complexes of the type *c*-$[Pd(\eta^3\text{-}C_3H_5)(pz^Rpy)]^+$ constitute the second example of calamitic materials based on cationic complexes containing *N*,*N*′-bidentate ligands [3].

2. Experimental

2.1. Materials and physical measurements

All commercial reagents were used as supplied. The starting Pd-complexes, $[Pd(Cl)_2(PhCN)_2]$ and $[Pd(\mu\text{-}Cl)(\eta^3\text{-}C_3H_5)]_2$, were purchased from Sigma–Aldrich and used as supplied.

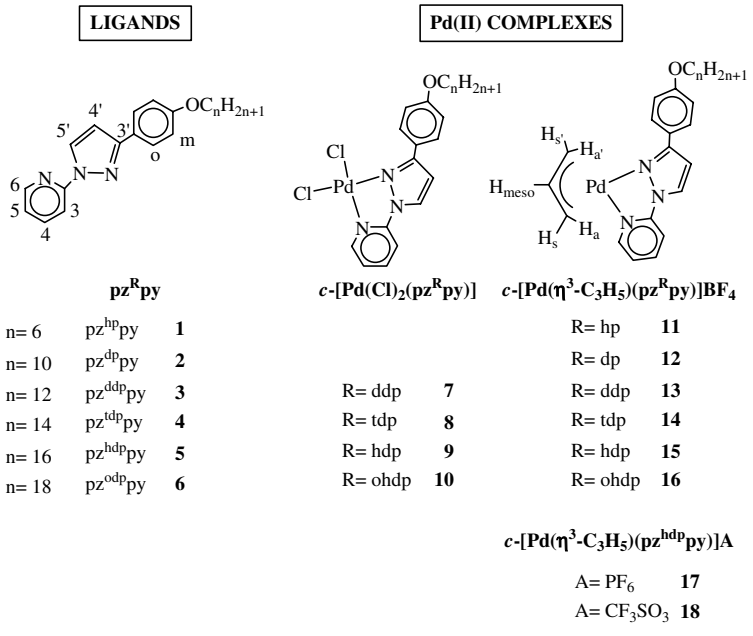

Scheme 1.

The 4-alkyloxyacetophenones were synthesised by alkylation of 4-hydroxyacetophenone with the corresponding *n*-alkyliodide in acetone solution of potassium carbonate as previously described [2,17]. All these compounds were characterised satisfactorily by analytical and spectroscopic techniques.

Elemental analyses for carbon, hydrogen, nitrogen and sulphur were carried out by the Microanalytical Service of the Complutense University. IR spectra were recorded on a FTIR Nicolet Magna-550 spectrophotometer with samples as KBr pellets in the 4000–400 cm^{-1} region: vs (very strong), s (strong), m (medium), w (weak).

^1H NMR spectra were performed on a Bruker AC-200 or on a Bruker DPX-300 spectrophotometers (NMR Service of the Complutense University) from solutions in $CDCl_3$. Chemical shifts δ are listed in ppm relative to TMS using the signal of the deuterated solvent as reference (7.26 ppm), and coupling constants J are in hertz. Multiplicities are indicated as s (singlet), d (doublet), t (triplet), m (multiplet), br s (broad signal). The atomic numbering used in the assignment of the NMR signals is shown in Scheme 1. The ^1H chemical shifts and coupling constants are accurate to ±0.01 ppm and ±0.3 Hz, respectively.

Phase studies were carried out by optical microscopy using an Olympus BX50 microscope equipped with a Linkam THMS 600 heating stage. The temperatures were assigned on the basis of optic observations with polarised light.

Measurements of the transition temperatures were made using a Perkin–Elmer Pyris 1 differential scanning calorimeter with the sample (1–4 mg) hermetically sealed in aluminium pans and with a heating or cooling rate of 5–10°/min.

2.2. Synthetic methods

2.2.1. Preparation of 2-[3-(4-alkyloxyphenyl)pyrazol-1-yl]pyridine (pz^Rpy, $R = C_6H_4OC_nH_{2n+1}$, $n = 6$ (hp), 10 (dp), 12 (ddp), 14 (tdp), 16 (hdp), 18 (odp)) (**1–6**)

A solution of 4-alkyloxyacetophenone (9.42 mmol) and ethyl formate (1.16 mL, 14.13 mmol) in toluene (15 mL) was added to a slurry of an excess of 60% sodium hydride (0.50 g, 12.5 mmol) in toluene (50 mL). A clear solution was obtained, which became a slurry after 5 min. The mixture was stirred overnight at room temperature and the solid was filtered and washed with dichloromethane and hexane. The solid obtained (1.48 mmol) was dissolved in ethanol 96% (10 mL), and acidified by dropwise addition of hydrochloric acid (ca. 2.5 mL, spec. grav. 1.18). 2-Hydrazinopyridine (0.65 g, 5.92 mmol) dissolved in the minimum amount of ethanol 96% was added to this solution. The mixture was refluxed for 3 h, and then the solvent was evaporated to ca. half the original volume and the resulting solution kept overnight at 4 °C. The solid obtained was filtered off, washed with hexane and dried in air. Yields and analytical data are given in Table 1.

$pz^{hp}py$ (***1***): IR (KBr, cm^{-1}): ν(CN) 1615 (vs), $\gamma(CH)_{py}$ 777 (m). ^1H NMR ($CDCl_3$, δ in ppm, J in Hz): 8.56 (d, $^3J = 2.6$, 1H, H5′), 8.41 (d, $^3J = 4.3$, 1H, H6), 8.08 (d, $^3J = 8.3$, 1H, H3), 7.85 (d, $^3J = 8.8$, 2H, H*o*), 7.80 (1H, H4), 7.17 (dd, $^3J = 7.4$, $^3J = 4.3$, 1H, H5), 6.96 (d, $^3J = 8.8$, 2H, H*m*), 6.72 (d, $^3J = 2.6$, 1H, H4′), 4.01 (t, $^3J = 6.6$, 2H, OCH_2), 1.81 (m, 2H, CH_2), 1.5–1.2 (m, 6H, CH_2), 0.91 (t, $^3J = 6.8$, 3H, CH_3).

$pz^{dp}py$ (***2***): IR (KBr, cm^{-1}): ν(CN) 1612 (vs), $\gamma(CH)_{py}$ 766 (s). ^1H NMR ($CDCl_3$, δ in ppm, J in Hz): 8.56 (d, $^3J = 2.7$, 1H, H5′), 8.41 (d, $^3J = 4.3$, 1H, H6), 8.08

Table 1
Yield and elemental analyses for the pz^Rpy ligands **1–6** and their Pd-complexes **7–18**

	Yield (%)	Molecular formula	Elemental analysis (%)		
			Found (calculated)		
			C	H	N
1	36	$C_{20}H_{23}N_3O$	74.4 (74.7)	7.5 (7.2)	13.1 (13.1)
2	45	$C_{24}H_{31}N_3O$	76.7 (76.4)	8.6 (8.3)	10.9 (11.1)
3	45	$C_{26}H_{35}N_3O$	76.9 (77.0)	8.8 (8.7)	10.5 (10.4)
4	55	$C_{28}H_{39}N_3O$	77.2 (77.6)	9.0 (9.1)	9.6 (9.7)
5	61	$C_{30}H_{43}N_3O$	77.9 (78.1)	9.3 (9.4)	9.0 (9.1)
6	47	$C_{32}H_{47}N_3O$	78.3 (78.5)	9.6 (9.7)	8.5 (8.6)
7	44	$C_{26}H_{35}PdCl_2N_3O \cdot 3/4CH_2Cl_2$	50.0 (49.7)	5.5 (5.7)	6.7 (6.5)
8	51	$C_{28}H_{39}PdCl_2N_3O \cdot 3/4CH_2Cl_2$	50.9 (51.2)	6.0 (6.1)	6.4 (6.2)
9	65	$C_{30}H_{43}PdCl_2N_3O$	56.6 (56.4)	6.6 (6.8)	6.7 (6.6)
10	66	$C_{32}H_{47}PdCl_2N_3O \cdot 1/3CH_2Cl_2$	55.9 (55.9)	6.9 (6.9)	6.3 (6.1)
11	44	$C_{23}H_{28}PdBF_4N_3O$	49.4 (49.7)	5.0 (5.1)	7.6 (7.6)
12	69	$C_{27}H_{36}PdBF_4N_3O$	52.7 (53.0)	5.8 (5.9)	6.8 (6.9)
13	44	$C_{29}H_{40}PdBF_4N_3O$	54.1 (54.4)	6.2 (6.3)	6.5 (6.6)
14	36	$C_{31}H_{44}PdBF_4N_3O \cdot 1/2CH_2Cl_2$	53.3 (53.3)	6.2 (6.4)	6.3 (6.0)
15	48	$C_{33}H_{48}PdBF_4N_3O$	57.3 (57.0)	6.9 (7.0)	6.1 (6.0)
16	36	$C_{35}H_{52}PdBF_4N_3O \cdot 1/2CH_2Cl_2$	55.8 (55.6)	6.8 (7.0)	5.7 (5.5)
17	25	$C_{33}H_{48}PdF_6N_3OP \cdot 1/4CH_2Cl_2$	51.2 (51.5)	6.2 (6.3)	5.6 (5.4)
18	36	$C_{34}H_{48}PdF_3N_3O_4S$[a]	53.9 (53.9)	6.4 (6.4)	5.5 (5.5)

[a] S: 4.4 (4.2).

(d, $^3J = 7.7$, 1H, H3), 7.84 (d, $^3J = 8.4$, 2H, H*o*), 7.80 (1H, H4), 7.17 (dd, $^3J = 7.6$, $^3J = 4.3$, 1H, H5), 6.96 (d, $^3J = 8.7$, 2H, H*m*), 6.72 (d, $^3J = 2.6$, 1H, H4′), 4.00 (t, $^3J = 6.5$, 2H, OCH_2), 1.88 (m, 2H, CH_2), 1.5–1.2 (m, 14H, CH_2), 0.89 (t, $^3J = 6.8$, 3H, CH_3).

pz^{ddp}py (***3***): IR (KBr, cm^{-1}): *ν*(CN) 1612 (vs), *γ*(CH)$_{py}$ 766 (s). ^{1}H NMR ($CDCl_3$, *δ* in ppm, *J* in Hz): 8.56 (d, $^3J = 2.8$, 1H, H5′), 8.40 (ddd, $^3J = 4.6$, $^4J = 2.0$, $^5J = 0.8$, 1H, H6), 8.08 (ddd, $^3J = 8.2$, $^4J = {}^5J = 1.0$, 1H, H3), 7.85 (d, $^3J = 8.8$, 2H, H*o*), 7.81 (ddd, $^3J = 8.4$, $^3J = 7.4$, $^4J = 2.0$, 1H, H4), 7.16 (ddd, $^3J = 7.4$, $^3J = 4.8$, $^4J = 1.0$, 1H, H5), 6.96 (d, $^3J = 9.0$, 2H, H*m*), 6.71 (d, $^3J = 2.6$, 1H, H4′), 4.00 (t, $^3J = 6.6$, 2H, OCH_2), 1.81 (m, 2H, CH_2), 1.5–1.2 (m, 18H, CH_2), 0.88 (t, $^3J = 6.8$, 3H, CH_3).

pz^{tdp}py (***4***): IR (KBr, cm^{-1}): *ν*(CN) 1613 (vs), *γ*(CH)$_{py}$ 766 (s). ^{1}H NMR ($CDCl_3$, *δ* in ppm, *J* in Hz): 8.58 (d, $^3J = 2.8$, 1H, H5′), 8.41 (ddd, $^3J = 4.8$, $^4J = 2.0$, $^5J = 1.0$, 1H, H6), 8.09 (ddd, $^3J = 8.2$, $^4J = {}^5J = 1.0$, 1H, H3), 7.86 (d, $^3J = 9.0$, 2H, H*o*), 7.82 (ddd, $^3J = 8.4$, $^3J = 7.4$, $^4J = 2.0$, 1H, H4), 7.17 (ddd, $^3J = 7.4$, $^3J = 4.8$, $^4J = 1.2$, 1H, H5), 6.96 (d, $^3J = 8.8$, 2H, H*m*), 6.72 (d, $^3J = 2.8$, 1H, H4′), 4.01 (t, $^3J = 6.6$, 2H, OCH_2), 1.81 (m, 2H, CH_2), 1.5–1.2 (m, 22H, CH_2), 0.88 (t, $^3J = 6.4$, 3H, CH_3).

pz^{hdp}py (***5***): IR (KBr, cm^{-1}): *ν*(CN) 1613 (vs), *γ*(CH)$_{py}$ 766 (s). ^{1}H NMR ($CDCl_3$, *δ* in ppm, *J* in Hz): 8.56 (d, $^3J = 2.8$, 1H, H5′), 8.41 (ddd, $^3J = 4.8$, $^4J = 2.0$, $^5J = 1.0$, 1H, H6), 8.08 (ddd, $^3J = 8.4$, $^4J = {}^5J = 1.0$, 1H, H3), 7.85 (d, $^3J = 8.8$, 2H, H*o*), 7.78 (ddd, $^3J = 8.4$, $^3J = 7.4$, $^4J = 2.0$, 1H, H4), 7.17 (ddd, $^3J = 7.2$, $^3J = 4.8$, $^4J = 1.0$, 1H, H5), 6.96 (d, $^3J = 8.8$, 2H, H*m*), 6.72 (d, $^3J = 2.8$, 1H, H4′), 4.00 (t, $^3J = 6.6$, 2H, OCH_2), 1.81 (m, 2H, CH_2), 1.5–1.2 (m, 26H, CH_2), 0.88 (t, $^3J = 6.6$, 3H, CH_3).

pz^{odp}py (***6***): IR (KBr, cm^{-1}): *ν*(CN) 1612 (vs), *γ*(CH)$_{py}$ 766 (s). ^{1}H NMR ($CDCl_3$, *δ* in ppm, *J* in Hz): 8.56 (d, $^3J = 2.8$, 1H, H5′), 8.41 (ddd, $^3J = 4.6$, $^4J = 2.0$, $^5J = 1.0$, 1H, H6), 8.08 (ddd, $^3J = 8.4$, $^4J = {}^5J = 1.0$, 1H, H3), 7.84 (d, $^3J = 8.8$, 2H, H*o*), 7.82 (ddd, $^3J = 8.4$, $^3J = 7.4$, $^4J = 2.0$, 1H, H4), 7.16 (ddd, $^3J = 7.2$, $^3J = 4.8$, $^4J = 1.0$, 1H, H5), 6.96 (d, $^3J = 8.8$, 2H, H*m*), 6.71 (d, $^3J = 2.8$, 1H, H4′), 4.01 (t, $^3J = 6.6$, 2H, OCH_2), 1.81 (m, 2H, CH_2), 1.5–1.2 (m, 30H, CH_2), 0.88 (t, $^3J = 6.8$, 3H, CH_3).

2.2.2. Preparation of c-[Pd(Cl)$_2$(pz^{R}py)] (R = $C_6H_4OC_nH_{2n+1}$, n = 12 (ddp), 14 (tdp), 16 (hdp), 18 (odp)) (***7–10***)

To a solution of the corresponding pz^{R}py ligand (0.130 mmol) in chloroform (10 mL) was added [Pd(Cl)$_2$(PhCN)$_2$] (50 mg, 0.130 mmol). The mixture of reaction was refluxed for 3 h and then let stirring overnight at room temperature. The solvent was removed and the solid recrystallised in dichloromethane/hexane leading to the precipitation of a yellow solid, which was filtered off, washed with hexane and dried in vacuo. Yields and analytical data are given in Table 1.

c-[Pd(Cl)$_2$(pz^{ddp}py)] (***7***): IR (KBr, cm^{-1}): *ν*(CN) 1612 (vs), *γ*(CH)$_{py}$ 772 (s). ^{1}H NMR ($CDCl_3$, *δ* in ppm, *J* in Hz): 9.01 (d, $^3J = 5.4$, 1H, H6), 8.45 (br s, 1H, H5′), 8.10 (dd, $^3J = 7.1$, 1H, H4), 7.77 (d, $^3J = 7.8$, 1H, H3), 7.62 (d, $^3J = 8.6$, 2H, H*o*), 7.31 (dd, $^3J = 6.3$, 1H, H5), 6.91 (d, $^3J = 8.6$, 2H, H*m*), 6.66 (br s, 1H, H4′), 3.98 (t, $^3J = 6.1$, 2H, OCH_2), 1.79 (m, 2H, CH_2), 1.5–1.2 (m, 18H, CH_2), 0.88 (t, $^3J = 6.8$, 3H, CH_3).

c-[Pd(Cl)$_2$(pz^{tdp}py)] (***8***): IR (KBr, cm^{-1}): *ν*(CN) 1612 (vs), *γ*(CH)$_{py}$ 772 (s). ^{1}H NMR ($CDCl_3$, *δ* in ppm, *J* in Hz): 9.06 (d, $^3J = 5.5$, 1H, H6), 8.38 (br s, 1H, H5′), 8.09 (dd, $^3J = 7.8$, 1H, H4), 7.69 (1H, H3), 7.63 (d, $^3J = 8.3$, 2H, H*o*), 7.33 (dd, $^3J = 6.8$, 1H, H5), 6.91 (d, $^3J = 8.3$, 2H, H*m*), 6.68 (br s, 1H, H4′), 3.99 (t, $^3J = 6.4$, 2H, OCH_2), 1.76 (m, 2H, CH_2), 1.5–1.2 (m, 22H, CH_2), 0.88 (t, $^3J = 6.3$, 3H, CH_3).

c-[Pd(Cl)$_2$(pz^{hdp}py)] (***9***): IR (KBr, cm^{-1}): *ν*(CN) 1612 (vs), *γ*(CH)$_{py}$ 771 (s). ^{1}H NMR ($CDCl_3$, *δ* in ppm, *J* in Hz): 9.07 (d, $^3J = 5.6$, 1H, H6), 8.35 (br s, 1H, H5′), 8.09 (dd, $^3J = 8.1$, 1H, H4), 7.68 (1H, H3), 7.64 (d, $^3J = 8.6$, 2H, H*o*), 7.33 (dd, $^3J = 7.1$, 1H, H5), 6.93 (d, $^3J = 8.6$, 2H, H*m*), 6.68 (br s, 1H, H4′), 3.99 (t, $^3J = 6.6$, 2H, OCH_2), 1.80 (m, 2H, CH_2), 1.5–1.2 (m, 26H, CH_2), 0.88 (t, $^3J = 6.6$, 3H, CH_3).

c-[Pd(Cl)$_2$(pz^{odp}py)] (***10***): IR (KBr, cm^{-1}): *ν*(CN) 1612 (vs), *γ*(CH)$_{py}$ 771 (s). ^{1}H NMR ($CDCl_3$, *δ* in ppm, *J* in Hz): 9.14 (d, $^3J = 5.5$, 1H, H6), 8.27 (d, $^3J = 2.9$, 1H, H5′), 8.09 (ddd, $^3J = 8.5$, $^3J = 7.4$, $^3J = 1.2$, 1H, H4), 7.66 (d, $^3J = 8.5$, 2H, H*o*), 7.60 (1H, H3), 7.36 (dd, $^3J = 6.3$, 1H, H5), 6.92 (d, $^3J = 8.5$, 2H, H*m*), 6.70 (d, $^3J = 2.9$, 1H, H4′), 3.99 (t, $^3J = 6.3$, 2H, OCH_2), 1.80 (m, 2H, CH_2), 1.5–1.2 (m, 30H, CH_2), 0.88 (t, $^3J = 6.8$, 3H, CH_3).

2.2.3. Preparation of c-[Pd(η^3-C_3H_5)(pz^{R}py)]BF$_4$ (R = $C_6H_4OC_nH_{2n+1}$, n = 6 (hp), 10 (dp), 12 (ddp), 14 (tdp), 16 (hdp), 18 (odp)) (***11–16***)

To a solution of [Pd(μ-Cl)(η^3-C_3H_5)]$_2$ (100 mg, 0.273 mmol) in dry acetone (20 mL) was added $AgBF_4$ (106.3 mg, 0.546 mmol) under nitrogen atmosphere. The mixture was stirred overnight in the absence of light and then filtered over Celite. The corresponding pz^{R}py (0.546 mmol) in dichloromethane (15 mL) was added to the resulting solution and let stirring overnight at room temperature. Then the solvent was removed in vacuo and the solid recrystallised in dichloromethane/hexane leading to the precipitation of a colorless solid, which was filtered off, washed with hexane and dried in vacuo. Yields and analytical data are given in Table 1.

c-[Pd(η^3-C_3H_5)(pz^{hp}py)]BF$_4$ (***11***): IR (KBr, cm^{-1}): *ν*(CN) 1609 (vs), *γ*(CH)$_{py}$ 777 (s), *ν*(BF) 1052 (vs), *δ* (FBF) 522 (w). ^{1}H NMR ($CDCl_3$, *δ* in ppm, *J* in Hz): 8.82 (d, $^3J = 2.7$, 1H, H5′), 8.57 (d, $^3J = 5.7$, 1H, H6), 8.26 (d, $^3J = 8.4$, 1H, H3), 8.17 (dd, $^3J = 8.4$, $^3J = 7.2$, 1H, H4), 7.50 (d, $^3J = 8.7$, 2H, H*o*), 7.43 (dd, $^3J = 7.0$, $^3J = 5.4$, 1H, H5), 7.02 (d, $^3J = 8.7$, 2H, H*m*), 6.79 (d, $^3J = 2.7$, 1H, H4′), 5.67 (m, $^3J_a = 12.5$, $^3J_s = 6.9$, 1H, H*meso*), 4.30 (br s, 1H, H*s*), 4.04 (t, $^3J = 6.6$, 2H, OCH_2), 3.8-3.0 (br s, 3H, H*s* + H*a*), 1.84 (m, 2H, CH_2), 1.5–1.2 (m, 6H, CH_2), 0.94 (t, $^3J = 6.9$, 3H, CH_3).

c-[Pd(η³-C₃H₅)(pz^dppy)]BF₄ (**12**): IR (KBr, cm^{-1}): ν(CN) 1611 (vs), $\gamma(CH)_{py}$ 783 (s), ν(BF) 1052 (vs), δ (FBF) 522 (w). ^1H NMR ($CDCl_3$, δ in ppm, *J* in Hz): 8.80 (d, $^3J = 2.9$, 1H, H5′), 8.58 (d, $^3J = 5.4$, 1H, H6), 8.29 (ddd, $^3J = 8.0$, $^3J = 7.3$, $^4J = 1.0$, 1H, H4), 8.23 (d, $^3J = 8.3$, 1H, H3), 7.49 (d, $^3J = 8.5$, 2H, H*o*), 7.42 (dd, $^3J = 7.0$, $^3J = 5.4$, 1H, H5), 7.02 (d, $^3J = 8.5$, 2H, H*m*), 6.77 (d, $^3J = 2.9$, 1H, H4′), 5.67 (m, $^3J_a = 12.5$, $^3J_s = 6.9$, 1H, H*meso*), 4.38 (br s, 1H, H*s*), 4.03 (t, $^3J = 6.5$, 2H, OCH_2), 3.59 (br s, 2H, H*s* + H*a*), 3.10 (br s, 1H, H*a*), 1.83 (m, 2H, CH_2), 1.6–1.2 (m, 14H, CH_2), 0.88 (t, $^3J = 6.8$, 3H, CH_3).

c-[Pd(η³-C₃H₅)(pz^ddppy)]BF₄ (**13**): IR (KBr, cm^{-1}): ν(CN) 1612 (vs), $\gamma(CH)_{py}$ 783 (s), ν(BF) 1056 (vs), δ (FBF) 523 (w). ^1H NMR ($CDCl_3$, δ in ppm, *J* in Hz): 8.82 (d, $^3J = 2.7$, 1H, H5′), 8.57 (d, $^3J = 5.4$, 1H, H6), 8.28 (d, $^3J = 8.3$, 1H, H3), 8.19 (dd, $^3J = 8.3$, $^3J = 7.8$, 1H, H4), 7.50 (d, $^3J = 8.5$, 2H, H*o*), 7.43 (dd, $^3J = 5.8$, 1H, H5), 7.02 (d, $^3J = 8.5$, 2H, H*m*), 6.79 (d, $^3J = 2.7$, 1H, H4′), 5.67 (m, $^3J_a = 12.4$, $^3J_s = 7.0$, 1H, H*meso*), 4.32 (br s, 1H, H*s*), 4.02 (t, $^3J = 6.1$, 2H, OCH_2), 3.55 (br s, 2H, H*s* + H*a*), 3.14 (br s, 1H, H*a*), 1.83 (m, 2H, CH_2), 1.5–1.2 (m, 18H, CH_2), 0.88 (t, $^3J = 6.8$, 3H, CH_3).

c-[Pd(η³-C₃H₅)(pz^tdppy)]BF₄ (**14**): IR (KBr, cm^{-1}): ν(CN) 1612 (vs), $\gamma(CH)_{py}$ 783 (s), ν(BF) 1056 (vs), δ (FBF) 523 (w). ^1H NMR ($CDCl_3$, δ in ppm, *J* in Hz): 8.83 (d, $^3J = 2.9$, 1H, H5′), 8.57 (d, $^3J = 5.1$, 1H, H6), 8.28 (d, $^3J = 8.3$, 1H, H3), 8.19 (dd, $^3J = 7.6$, 1H, H4), 7.50 (d, $^3J = 8.6$, 2H, H*o*), 7.43 (dd, $^3J = 6.1$, 1H, H5), 7.02 (d, $^3J = 8.6$, 2H, H*m*), 6.80 (d, $^3J = 2.9$, 1H, H4′), 5.67 (m, $^3J_a = 12.4$, $^3J_s = 6.9$, 1H, H*meso*), 4.03 (t, $^3J = 6.6$, 3H, OCH_2 + H*s*), 3.31 (br s, 3H, H*s* + H*a*), 1.84 (m, 2H, CH_2), 1.5-1.2 (m, 22H, CH_2), 0.88 (t, $^3J = 6.6$, 3H, CH_3).

c-[Pd(η³-C₃H₅)(pz^hdppy)]BF₄ (**15**): IR (KBr, cm^{-1}): ν(CN) 1612 (vs), $\gamma(CH)_{py}$ 781 (s), ν(BF) 1053 (vs), δ (FBF) 522 (w). ^1H-NMR ($CDCl_3$, δ in ppm, *J* in Hz): 8.81 (d, $^3J = 2.9$, 1H, H5′), 8.58 (d, $^3J = 4.9$, 1H, H6), 8.25 (d, $^3J = 8.3$, 1H, H3), 8.14 (dd, $^3J = 8.3$, $^3J = 7.3$, 1H, H4), 7.50 (d, $^3J = 8.6$, 2H, H*o*), 7.42 (dd, $^3J = 6.4$, 1H, H5), 7.02 (d, $^3J = 8.6$, 2H, H*m*), 6.78 (d, $^3J = 2.9$, 1H, H4′), 5.67 (m, $^3J_a = 12.5$, $^3J_s = 6.8$, 1H, H*meso*), 4.12 (br s, 1H, H*s*), 4.03 (t, $^3J = 6.6$, 2H, OCH_2), 3.32 (br s, 2H, H*s* + H*a*), 3.04 (br s, 1H, H*a*), 1.83 (m, 2H, CH_2), 1.5–1.2 (m, 26H, CH_2), 0.94 (t, $^3J = 6.9$, 3H, CH_3).

c-[Pd(η³-C₃H₅)(pz^odppy)]BF₄ (**16**): IR (KBr, cm^{-1}): ν(CN) 1612 (vs), $\gamma(CH)_{py}$ 783 (s), ν(BF) 1056 (vs), δ (FBF) 523 (w). ^1H NMR ($CDCl_3$, δ in ppm, *J* in Hz): 8.82 (d, $^3J = 2.9$, 1H, H5′), 8.57 (d, $^3J = 5.1$, 1H, H6), 8.27 (d, $^3J = 8.3$, 1H, H3), 8.17 (d, $^3J = 7.8$, 1H, H4), 7.50 (d, $^3J = 8.8$, 2H, H*o*), 7.45 (dd, $^3J = 6.1$, 1H, H5), 7.02 (d, $^3J = 8.8$, 2H, H*m*), 6.79 (d, $^3J = 2.9$, 1H, H4′), 5.67 (m, $^3J_a = 12.4$, $^3J_s = 6.9$, 1H, H*meso*), 4.03 (t, $^3J = 6.3$, 3H, OCH_2 + H*s*), 3.31 (br s, 3H, H*s* + H*a*), 1.83 (m, 2H, CH_2), 1.5–1.2 (m, 30H, CH_2), 0.88 (t, $^3J = 6.6$, 3H, CH_3).

2.2.4. Preparation of *c-[Pd(η³-C₃H₅)(pz^hdppy)]A* (*A = PF₆* **17**, *CF₃SO₃* **18**)

These compounds were prepared by the same way to that of $[Pd(\eta^3\text{-}C_3H_5)(pz^Rpy)]BF_4$, starting from $[Pd(\mu\text{-}Cl)(\eta^3\text{-}C_3H_5)]_2$ (50 mg, 0.137 mmol), $AgPF_6$ (69.3 mg, 0.274 mmol) or $AgCF_3SO_3$ (70.4 mg, 0.274 mmol), and $pz^{hdp}py$ (126.5 mg, 0.274 mmol). Yields and analytical data are given in Table 1.

c-[Pd(η³-C₃H₅)(pz^hdppy)]PF₆ (**17**): IR (KBr, cm^{-1}): ν(CN) 1612 (vs), $\gamma(CH)_{py}$ 780 (s), ν(PF) 838 (vs), δ (FPF) 557 (w). ^1H NMR ($CDCl_3$, δ in ppm, *J* in Hz): 8.57 (d, $^3J = 2.9$, 2H, H5′ + H6), 8.15 (dd, $^3J = 8.0$, $^3J = 7.0$, 1H, H4), 8.03 (d, $^3J = 8.3$, 1H, H3), 7.50 (d, $^3J = 8.5$, 2H, H*o*), 7.43 (dd, $^3J = 6.3$, 1H, H5), 7.02 (d, $^3J = 8.5$, 2H, H*m*), 6.79 (d, $^3J = 2.9$, 1H, H4′), 5.67 (m, $^3J_a = 12.6$, $^3J_s = 6.8$, 1H, H*meso*), 4.33 (br s, 1H, H*s*), 4.03 (t, $^3J = 6.6$, 2H, OCH_2), 3.55 (br s, 2H, H*s* + H*a*), 3.16 (br s, 1H, H*a*), 1.83 (m, 2H, CH_2), 1.5–1.1 (m, 26H, CH_2), 0.88 (t, $^3J = 6.6$, 3H, CH_3).

c-[Pd(η³-C₃H₅)(pz^hdppy)]CF₃SO₃ (**18**): IR (KBr, cm^{-1}): ν(CN) 1611 (vs), $\gamma(CH)_{py}$ 773 (s), $\nu(SO_3) + \nu(CF_3)$ 1257 (vs). ^1H NMR ($CDCl_3$, δ in ppm, *J* in Hz): 9.02 (d, $^3J = 2.9$, 1H, H5′), 8.57 (d, $^3J = 4.6$, 1H, H6), 8.45 (d, $^3J = 8.3$, 1H, H3), 8.23 (ddd, $^3J = 8.5$, $^3J = 7.3$, $^4J = 1.5$, 1H, H4), 7.51 (d, $^3J = 8.6$, 2H, H*o*), 7.45 (dd, $^3J = 6.3$, 1H, H5), 7.02 (d, $^3J = 8.6$, 2H, H*m*), 6.81 (d, $^3J = 2.9$, 1H, H4′), 5.68 (m, $^3J_a = 12.7$, $^3J_s = 6.8$, 1H, H*meso*), 4.04 (t, $^3J = 6.3$, 3H, OCH_2 + H*s*), 3.33 (br s, 3H, H*s* + H*a*), 1.84 (m, 2H, CH_2), 1.5–1.1 (m, 26H, CH_2), 0.89 (t, $^3J = 6.8$, 3H, CH_3).

2.3. X-ray structure determinations of *c-[Pd(η³-C₃H₅)-(pz^Rpy)]BF₄* (*R = hp* **11**, *dp* **12**)

Suitable colorless crystals of *c*-$[Pd(\eta^3\text{-}C_3H_5)(pz^{hp}py)]$-$BF_4$ (**11**) and *c*-$[Pd(\eta^3\text{-}C_3H_5)(pz^{dp}py)]BF_4$ (**12**) were grown by layering dichloromethane solutions with hexane. The crystals were mounted on a Smart CCD-Bruker diffractometer with graphite monochromated Mo-Kα radiation (λ = 0.71073 Å) operating at 50 kV and 20–25 mA. A summary of the fundamental crystal and refinement data for these structures is given in Table 2.

In both cases, data were collected over an hemisphere of the reciprocal space by combination of the three exposure sets. Each exposure of 20 s covered 0.3° in ω. The cell parameters were determined and refined by a least-squares fit of all reflections. The first 50 frames were recollected at the end of the data collection to monitor crystal decay, and no appreciable decay was observed. The structures were solved by direct methods and conventional Fourier techniques and refined by full-matrix least-squares on F^2 [18]. Anisotropic parameters were used in the last cycles of refinement for all non-hydrogen atoms with some exceptions. In both compounds, a non-resolvable disorder of the fluorine atoms of the BF_4 group and some carbon atoms was found. The F-atoms were included in two isotropical cycles for **12** and three anisotropical cycles for

Table 2
Crystal and refinement data for *c*-[Pd(η^3-C_3H_5)(pz^Rpy)]BF_4 (R = hp **11**, dp **12**)

	11	**12**
Empirical formula	$C_{23}H_{28}BF_4N_3OPd$	$C_{27}H_{36}BF_4N_3OPd$
Formula weight	555.69	611.80
Crystal system	Monoclinic	Monoclinic
Space group	$P2_1/c$	$P2_1/c$
a (Å)	17.607(1)	21.034(2)
b (Å)	9.8589(8)	9.809(1)
c (Å)	14.763(1)	14.928(2)
β (°)	103.578(2)	108.571(2)
V (Å^3)	2491.1(4)	2919.4(6)
Z	4	4
T (K)	293(2)	296(2)
$F(000)$	1128	1256
$\rho_{calc.}$ (g cm^{-3})	1.482	1.392
μ (mm^{-1})	0.794	0.685
Crystal dimensions (mm)	0.36 × 0.12 × 0.08	0.40 × 0.10 × 0.07
Scan technique	ω and ϕ	ω and ϕ
Data collected	(−23,−12,−17) to (23,13,19)	(−25,−11,−11) to (24,11,17)
θ range (°)	1.19–28.94	2.04–25.00
Reflections collected	15,554	14,845
Independent reflections	5936 (R_{int} = 0.0707)	5135 (R_{int} = 0.0809)
Data/restraints/parameters	5936/5/221	5135/12/227
Observed reflections [$I \geqslant 2\sigma(I)$]	2136	1757
R[a]	0.053	0.093
Rw_F[b]	0.165	0.302
Largest residual peak (e Å^{-3})	0.701	1.305

[a] $\sum[|F_o| - |F_c|]/\sum|F_o|$.
[b] $\{\sum[w(F_o^2 - F_c^2)^2]/\sum[w(F_o^2)^2]\}^{1/2}$.

11, and in subsequent cycles their thermal parameters were kept constant. Besides, analogous refinement was applied for the carbon atoms of the decyl chain and the allyl group in **12**, and for the carbon atoms of the hexyl chain in **11**. These carbon atoms were also refined with geometrical restraints and a variable common carbon–carbon distance. Hydrogen atoms were included in calculated positions and refined as riding on their respective carbon atoms. The refinement converged to R values of 0.053 and 0.093 for **11** and **12**, respectively.

The largest residual peaks in the final difference map were 0.701 and 1.305 e Å^{-3} for **11** and **12**, respectively, in the vicinity of the fluorine atoms of the BF_4 group. The supplementary crystallographic data have been passed to the Cambridge Crystallographic Data Centre (CCDC deposition numbers 275433 and 275434 for **11** and **12**, respectively).

3. Results and discussion

3.1. Synthetic and characterisation studies

The new ligands 2-[3-(4-alkyloxyphenyl)pyrazol-1-yl]pyridine (pz^Rpy; R = $C_6H_4OC_nH_{2n+1}$, n = 6 (hp), 10 (dp), 12 (ddp), 14 (tdp), 16 (hdp), 18 (odp)) (**1**–**6**) were prepared by reaction of the sodium salt of the corresponding 3-(4-alkyloxypropane)-1,3-dione and 2-hydrazinopyridine in a HCl/EtOH media in a same way to related compounds [3,19,20] (Scheme 2).

The reaction of the ligands **1**–**6** and $[Pd(Cl)_2(PhCN)_2]$ or [Pd(η^3-C_3H_5)(acetone)$_2$]BF_4 (prepared in situ by reaction of the dimer [Pd(μ-Cl)(η^3-C_3H_5)]$_2$ and $AgBF_4$ in acetone [21]) gave rise to the new compounds *c*-[Pd(Cl)$_2$(pz^Rpy)] (R = $C_6H_4OC_nH_{2n+1}$, n = 12, 14, 16, 18) (**7**–**10**) and *c*-[Pd(η^3-C_3H_5)(pz^Rpy)]BF_4 (R = $C_6H_4OC_nH_{2n+1}$, n = 6, 10, 12, 14, 16, 18) (**11**–**16**) (Scheme 2). Both ligands and compounds were characterised by analytical and spectroscopic techniques (IR and ^{1}H NMR), and all data agree with their proposed molecular formulation. Some Pd-compounds exhibit crystallisation solvent (dichloromethane) detected by elemental analysis and by ^{1}H NMR through a signal at 5.32 ppm, which was not removed even after large periods in vacuo.

The ^{1}H NMR spectra of the ligands **1**–**6** and complexes **7**–**18**, recorded in $CDCl_3$ solution at room temperature (see Section 2), show all the expected signals from the pyrazole and pyridine groups as well as those from the alkyloxyphenyl substituent. Some resonances appear to be overlapped or masked by other signals. The main difference in each series of compounds is the integration of the $(CH_2)_n$ signal.

In relation to the pyrazole groups, the H4′ and the alkyl chain protons are scarcely modified in the complexes compared with those from the free ligands. By contrast, the pyridine and phenyl protons are markedly displaced upon complexation. The most significant shift is produced for the H6 proton of the pyridine moiety, which is downfield moved by ca. 0.6 ppm from the free ligand (ca.

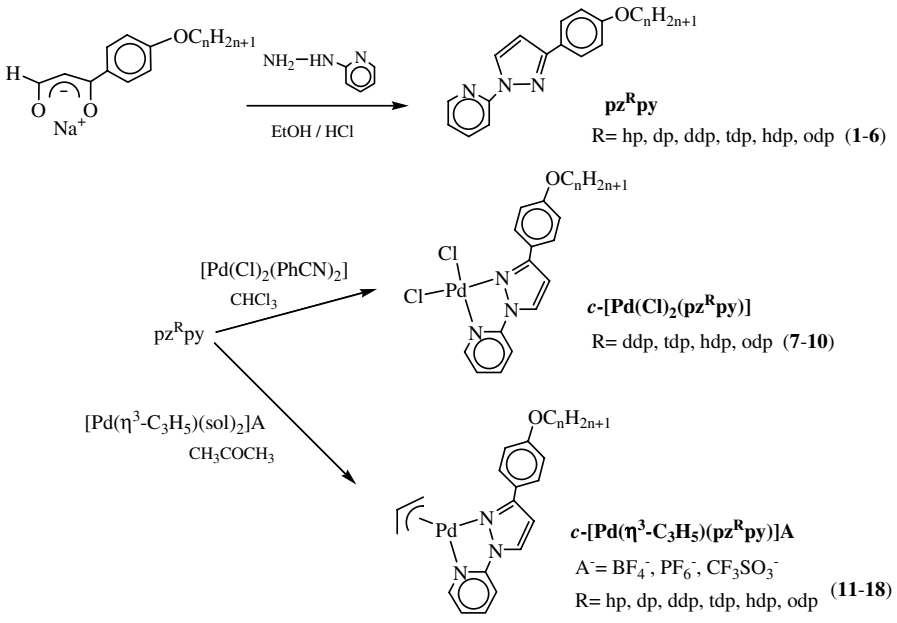

Scheme 2.

8.40 ppm) to the $PdCl_2$ derivatives (ca. 9.00 ppm), while for *c*-[Pd(η^3-C_3H_5)(pz^Rpy)]BF_4 the related shift is only ca. 0.15 ppm. The above result could be explained by considering the presence of interactions between the H6 proton and the neighbouring Pd-bonded chloride ligand.

On the other hand, the H*o* protons from the phenyl susbtituents at the pyrazole are upfield shifted by ca. 0.35 and 0.20 ppm on the *c*-[Pd(η^3-C_3H_5)(pz^Rpy)]BF_4 and *c*-[Pd$(Cl)_2$(pz^Rpy)] complexes, respectively.

For *c*-[Pd(η^3-C_3H_5)(pz^Rpy)]BF_4, the asymmetry of the compound accounts for a non-symmetrical allyl ligand, which determines the presence of two signals each *syn* and *anti* protons. These signals appear as three broad resonances at ca. 4.3 (H*s*), 3.6 (H*s* + H*a*) and 3.1 (H*a*) ppm, as a characteristic of a dynamic behaviour from the allyl group. There are many examples in the literature describing the dynamic behaviour of allylpalladium complexes [21–24]. A multiplet at 5.67 ppm for the *meso* proton, from which are determined the corresponding coupling constants, is also observed.

NMR experiments at variable temperature (from −50 to 50 °C) have been undertaken. However they proved to be unsuccessful, the allyl signals being not resolved.

3.2. X-ray crystal structures of c-[Pd(η^3-C_3H_5)(pz^Rpy)]BF_4 (R = hp **11**, dp **12**)

Suitable crystals of compounds **11** and **12** were obtained from dichloromethane/hexane solutions. Figs. 1 and 2 illustrate the molecular geometry of both compounds, and Table 3 lists selected bond distances and angles. Both compounds behave almost isostructural, showing only slight differences. They crystallise in the monoclinic system, $P2_1/c$ space group, with one [Pd(η^3-C_3H_5)(pz^Rpy)]BF_4 per asymmetric unit.

Due to the non-resolvable disorder found specially in **12** (see Section 2), we will only comment the crystal structure of **11**. However, as we have stated before, both compounds are isostructural and therefore the conclusions deduced for **11** can also be applied to **12**.

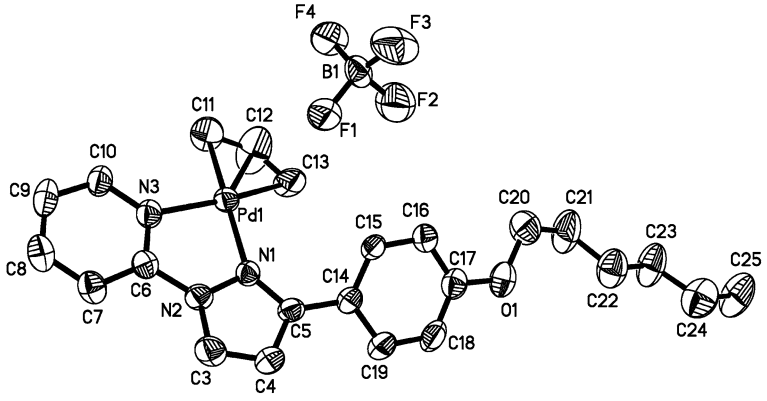

Fig. 1. ORTEP plot of **11** with 30% probability. Hydrogen atoms have been omitted for clarity.

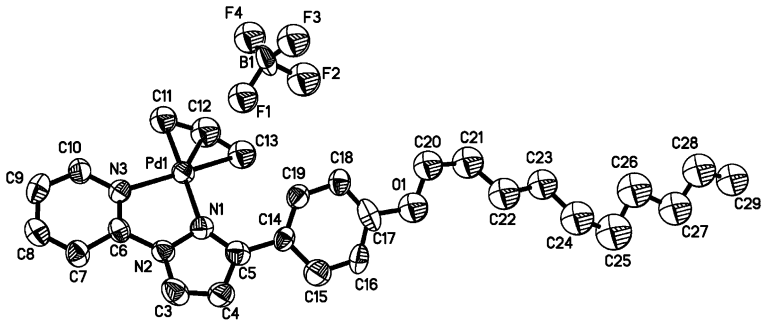

Fig. 2. ORTEP plot of **12** with 30% probability. Hydrogen atoms have been omitted for clarity.

Table 3
Selected bond distances (Å) and angles (°) for *c*-[Pd(η^3-C_3H_5)(pz^Rpy)]BF_4 (R = hp **11**, dp **12**)

	11	**12**
Pd1–N1	2.117(5)	2.11(1)
Pd1–N3	2.095(5)	2.10(1)
Pd1–C11	2.088(7)	2.15(2)
Pd1–C12	2.073(7)	2.12(2)
Pd–C13	2.105(7)	2.21(2)
C11–C12	1.244(11)	1.380(5)
C12–C13	1.193(11)	1.375(5)
B1–F1	1.354(9)	1.34(2)
B1–F2	1.412(10)	1.36(2)
B1–F3	1.291(8)	1.32(2)
B1–F4	1.310(8)	1.22(2)
N1–Pd–N3	77.8(2)	78.4(4)
N1–Pd–C11	176.8(3)	178.5(5)
N1–Pd1–C12	143.5(3)	143.3(5)
N1–Pd1–C13	110.3(2)	106.6(5)
N3–Pd1–C11	103.7(3)	100.4(5)
N3–Pd1–C12	138.3(3)	137.1(5)
N3–Pd1–C13	169.9(3)	171.6(5)
C11–Pd1–C12	34.8(3)	37.8(2)
C11–Pd1–C13	67.9(3)	74.5(3)
C12–Pd1–C13	33.2(3)	36.9(2)
C11–C12–C13	148.1(9)	147(2)
F1–B1–F2	102.8(7)	102(2)
F1–B1–F3	115.6(7)	116(1)
F1–B1–F4	112.1(6)	118(1)
F2–B1–F3	102.7(7)	90(1)
F2–B1–F4	104.4(7)	103(2)
F3–B1–F4	117.0(8)	120(2)

The geometry about the palladium(II), in the cationic entity, is distorted square-planar, the Pd atom deviating 0.081(1) Å of the N1N3C11C13 plane. The square-planar geometry can also be established by the dihedral angle of 6.0(3)° defined by the Pd1N1N3 and Pd1C11C13 planes.

The Pd–N distances (mean value of 2.101(5) Å) are similar to those found in related compounds [21,22,25,26]. The Pd–N1 and Pd–N3 bonds form the basis of the five-membered chelate ring, the Pd–N3 distance (2.095(5) Å) being slightly shorter than the Pd–N1 one (2.117(5) Å) in accordance with the expected difference in basicity of their respective heterocycles.

The allyl group C11C12C13 shows C–C bond distances of ca. 1.22 Å and a C–C–C angle of 148(1)°, which deviate from the ideal allyl geometry (ca. 1.36 Å and 120°, respectively). Similar distorted allyl groups have also been found in other complexes containing [Pd(η^3-allyl)]$^+$ fragments [25,27–30]. The Pd–C(allyl) distances (2.07–2.10 Å) are in the expected range for a [Pd(η^3-allyl)]$^+$ fragment with nitrogen ligands in *trans* position [21,22,26]. The Pd–C11 distance (2.088(8) Å) is slightly shorter than the Pd–C13 one (2.105(7) Å), this feature being related to a different *trans* influence of the N-coordinated heterocycle.

The dihedral angle between the allyl plane (C11C12C13) and the coordination plane defined by the Pd, N1 and N3 atoms is 3(1)°, with the allyl carbon atoms displaced a mean value of 0.16 Å with respect to this PdN1N3 plane.

The pyrazole and pyridine planes are almost parallel (dihedral angle of 4.4(2)°), defining an almost planar core of the cationic entity. However, the benzene plane from the substituent is twisted 33.5(3)° with respect to the own pyrazole plane.

The distorted tetrahedral BF_4^- counterion (mean B–F distance and F–B–F angle of 1.34(1) Å and 109.1(7)°, respectively) shows an interaction with the cationic unit through a weak coordinative Pd$\cdots$F1 contact of 3.543(6) Å.

To a supramolecular level, each [Pd(η^3-C_3H_5)(pz^{hp}py)]-BF_4 entity interacts with the neighbour through a weak non-conventional hydrogen bond C7$\cdots$F3 ($-x+1$, $y-1/2$, $-z+1/2$) of 3.08(1) Å, the molecules implicated showing a head-to-tail orientation. In such a way these interactions, which are propagated along the *b*-axis, give rise to a *zig-zag* chain (Fig. 3).

The interactions are further extended between the chains which are held together through a non-conventional hydrogen bond C9$\cdots$F1 ($-x+1$, $-y+2$, $-z+1$) of 3.271(8) Å. Additional non-covalent interactions that correspond to face-to-face $\pi\cdots\pi$ contacts between aromatic pyridine and benzene rings residing on the nearest neighbouring chains are also observed. The groups associated with the $\pi\cdots\pi$ interactions show the shortest separation of ca. 3.5 Å, which is consistent with that between heterocyclic ligands observed in several compounds [31–33]. The interchain interactions so defined give rise to layers, which are located almost parallel to the *bc* plane and generating a ^{2}D network (Fig. 4).

In this layered model, we could also consider that each molecule, which has a molecular geometry typical of

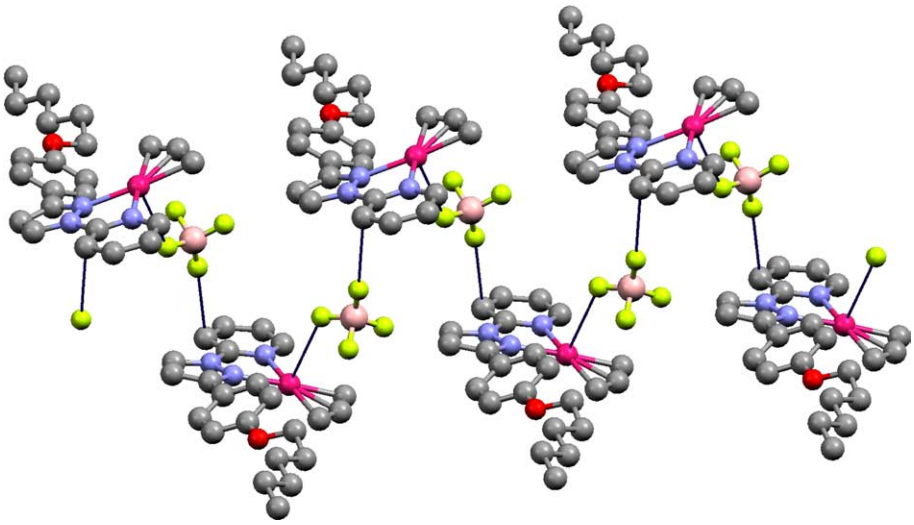

Fig. 3. View of the chain of **11** along the *b*-axis.

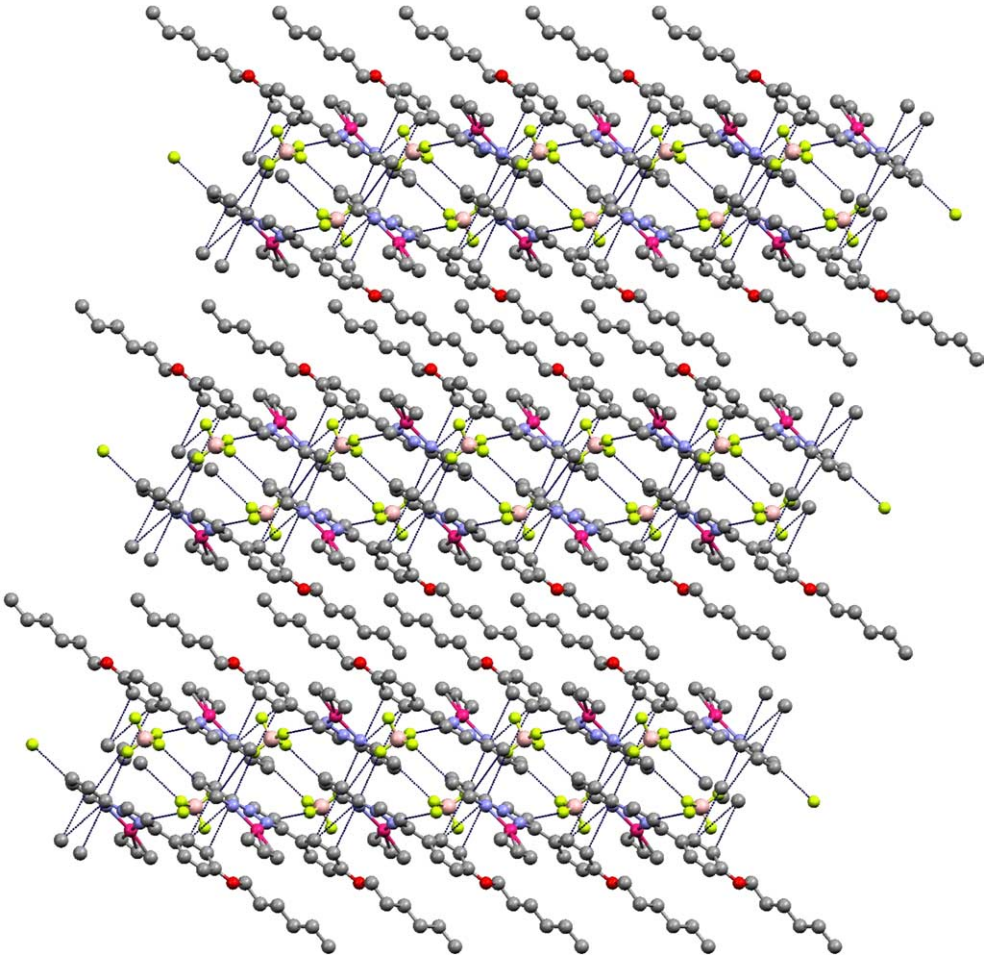

Fig. 4. ^{2}D network of **11**.

a rod-like shape, is associated by $\pi\cdots\pi$ interactions with molecules of neighbouring chains at 3.5 Å as well as with molecules of the own chain through the BF_4^- counterions, giving rise such an ordering related with a favourable dipole–dipole interaction (Fig. 4). The flexible chains of contiguous layers are interdigitated, leading to a global order which can be related to a lamellar interdigitated supramolecular organisation.

3.3. Thermal studies

The thermal behaviour of the pz^Rpy ligands (**1**–**6**) and their corresponding complexes *c*-$[Pd(Cl)_2(pz^Rpy)]$ (**7**–**10**) and *c*-$[Pd(\eta^3\text{-}C_3H_5)(pz^Rpy)]BF_4$ (**11**–**16**) have been studied by polarised optical microscopy (POM), differential scanning calorimetry (DSC) and variable-temperature X-ray diffraction (XRD).

Unlike their 3,5-disubstituted pyrazolylpyridine ($pz^{R2}py$) counterparts which showed monotropic smectic A mesophases [3], none of the new ligands pz^Rpy containing 3-substituted pyrazole groups displayed mesomorphism. These ligands were coordinated to the $PdCl_2$ group to give rise to the complexes *c*-$[Pd(Cl)_2(pz^Rpy)]$, which again did not exhibit liquid crystal properties at difference to their mesomorphic homologues *c*-$[Pd(Cl)_2(pz^{R2}py)]$ [3]. The above results appear to suggest that the vanishing of the liquid crystal properties in both cases, in relation to the 3,5-disubstituted counterparts, could be a reflect of the shortening of the molecular length maintaining the same width (Fig. 5).

However, the possibility of tuning the mesogenic properties, not only varying the length of the chains of the pyrazolylpyridine-type ligands but also the nature of metal fragment to which it is coordinated, moved us to extend the studies to those complexes containing $[Pd(\eta^3\text{-}C_3H_5)]^+$ as metal group. So, the thermal properties of the new complexes of the type *c*-$[Pd(\eta^3\text{-}C_3H_5)(pz^Rpy)]^+$ ($R = C_6H_4\text{-}OC_nH_{2n+1}$, $n = 6$ (hp), 10 (dp), 12 (ddp), 14 (tdp), 16 (hdp), 18 (odp)) containing BF_4^- as counterion (**11**–**16**) were investigated.

The complexes with a chain from 12 to 18 carbon atoms (**13**–**16**) display liquid crystal properties exhibiting mesophases with homeotropic and fan-shaped textures, which were identified as smectic A mesophases. Figs. 6(a) and (b) show textures of mesophases observed for some derivatives as representative examples. The transition temperatures as well as the corresponding enthalpies were determined by DSC and are given in Table 4. As general behaviour decomposition was observed after the mesophase was formed, and that decomposition was extensive after clearing.

In particular, complexes **13**–**16** show, on first heating, a crystal–crystal transition in the range of 60–95 °C, followed by a unidentified phase at ca. 140 °C. The observed viscosity of this phase by POM agrees with either a highly ordered phase or a soft crystal. After ca. 160 °C, a smectic A mesophase is identified which clears with decomposition at temperatures higher than 200 °C (Table 4). Typical DSC thermogram is depicted in Fig. 7(a) showing these features.

To determine the solidification temperature avoiding the decomposition, the samples were heated only at temperatures close to the formation of the mesophase and then they were cooled (Fig. 7(b)). Thus, the crystal–smectic A transition (ca. 160 °C) on heating was followed by the formation of the solid (ca. 130 °C) on cooling. Thermograms from second and successive heatings were identical showing only one transition from solid to mesophase (Fig. 7(b)).

As a general result, DSC analysis indicates that the *c*-$[Pd(\eta^3\text{-}C_3H_5)(pz^Rpy)]BF_4$ complexes essentially exhibit temperature-dependent polymorphism. These phase changes take the form of crystal–crystal transitions that are only observed on the first heating cycle. The second of these transitions generally exhibits smaller enthalpies than the third one (corresponding to the mesophase formation) (Table 4), suggesting that the second intermediate phase in these materials is crystalline rather than mesogenic instead of its slight softness observed by POM.

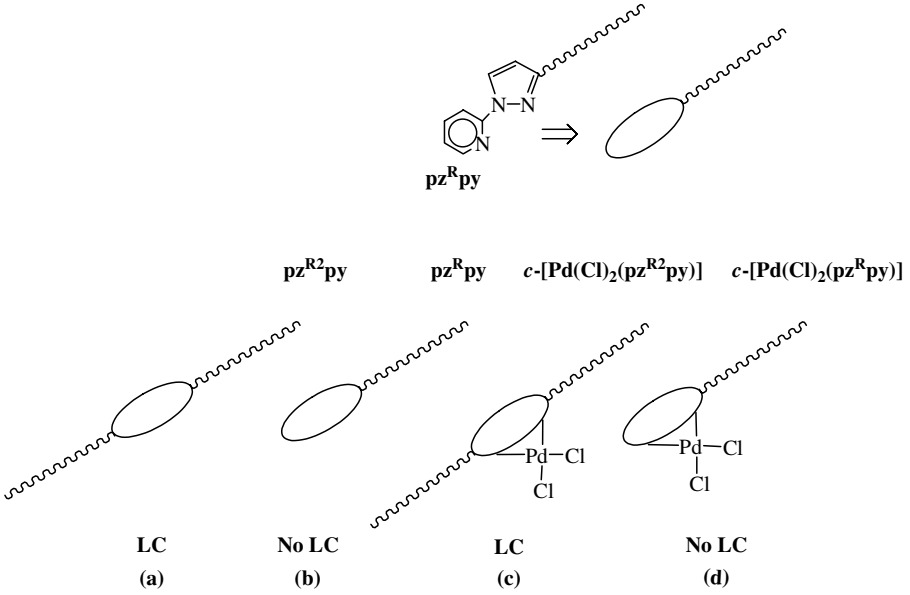

Fig. 5. Schematic molecular representation of the $pz^{R2}py$ (a) and pz^Rpy (b) ligands and their $PdCl_2$ complexes, *c*-$[Pd(Cl)_2(pz^{R2}py)]$ (c) and *c*-$[Pd(Cl)_2(pz^Rpy)]$ (d), showing the relationship of the molecular length.

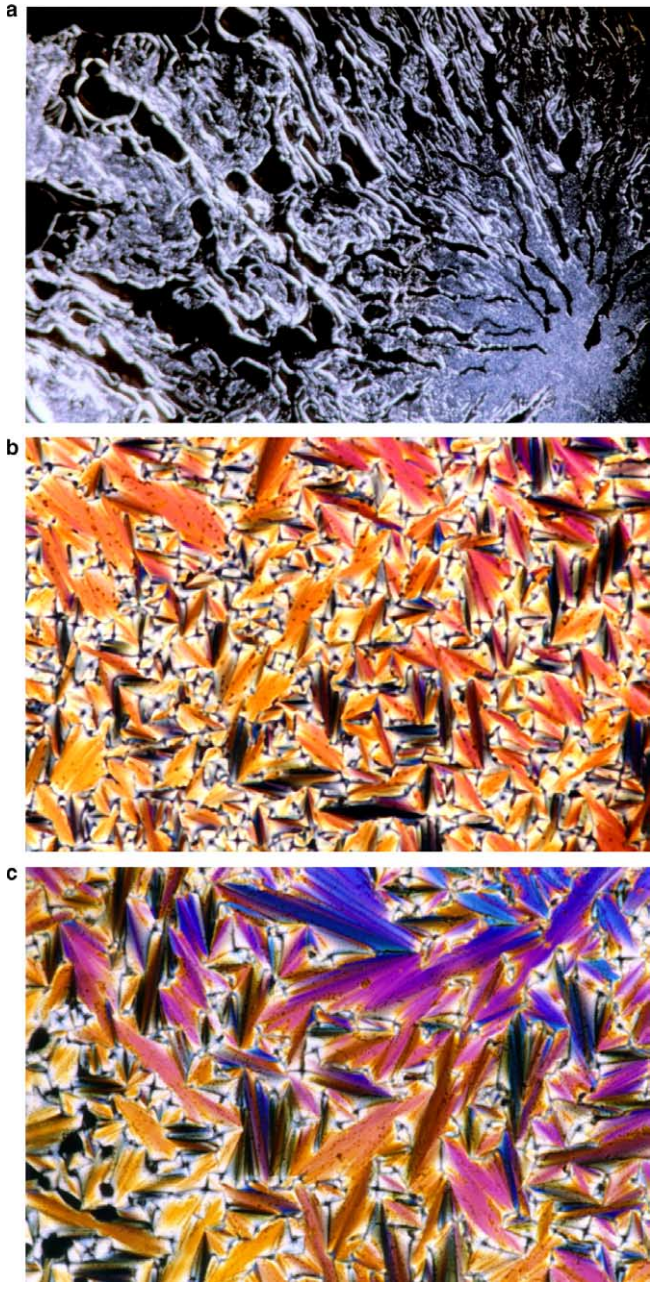

Fig. 6. Textures of the smectic A mesophase, observed on cooling, for: (a) compound **13** at 178 °C; (b) compound **15** at 180 °C; (c) compound **17** at 156 °C.

In order to get a better understanding of the nature of these thermotropic transitions, we have examined the phase behaviour of one representative complex *c*-[Pd(η^3-C_3H_5)(pz^{hdp}py)]BF_4 (**15**) by variable-temperature XRD. The results confirm the crystalline nature of the two first morphs on first heating cycle as well as the smectic mesophase produced after the third transition (Fig. 8(a)). In agreement with its assignation as smectic mesophase, the XRD pattern exhibits a low-angles sharp reflection (Fig. 8(a)) and a broad peak at wide-angles (Fig. 8(b)), which is consistent with a smectic-type layered structure that shows a *d*-spacing of 43.34 Å. For this compound

Table 4
Phase properties of *c*-[Pd(η^3-C_3H_5)(pz^Rpy)]BF_4 (R = hp, dp, ddp, tdp, hdp, odp) (**11**–**16**)

	Transition	*T* (°)	ΔH (kJ mol^{-1})
11 (hp)	Crys → I	175.0	15.7
12 (dp)	Crys → I	169.2	18.2
13 (ddp)	Crys → Crys′	93.6	11.0
	Crys′ → Crys″	134.3	9.9
	Crys″ → SmA	150.4	4.7
	SmA → I[a]	253.7	1.6
14 (tdp)	Crys → Crys′	61.5	12.5
	Crys′ → Crys″	148.4	8.1
	Crys″ → SmA	162.6	11.8
	SmA → I[a]	209.8	0.5
15 (hdp)	Crys → Crys′	79.3	16.2
	Crys′ → Crys″	134.9	11.5
	Crys″ → SmA	169.2	15.0
	SmA → I[a]	244.0	1.7
16 (odp)	Crys → Crys′	90.8	20.6
	Crys′ → Crys″	132.4	13.2
	Crys″ → SmA	156.2	15.7
	SmA → I[a]	~240[b]	

[a] Decomposition.
[b] Observed by polarised optical microscopy (POM).

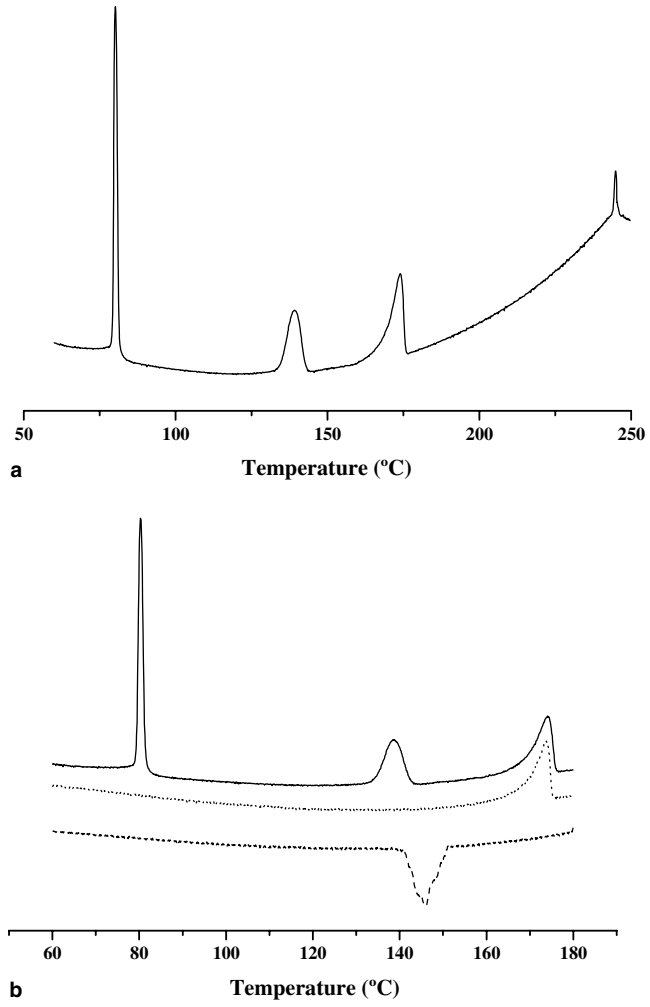

Fig. 7. DSC thermograms for *c*-[Pd(η^3-C_3H_5)(pz^{hdp}py)]BF_4 (**15**) in (a) the 50–250 °C range (first heating), and (b) the 50–180 °C range: first heating (straight line), first cooling (dashed line) and second heating (dotted line).

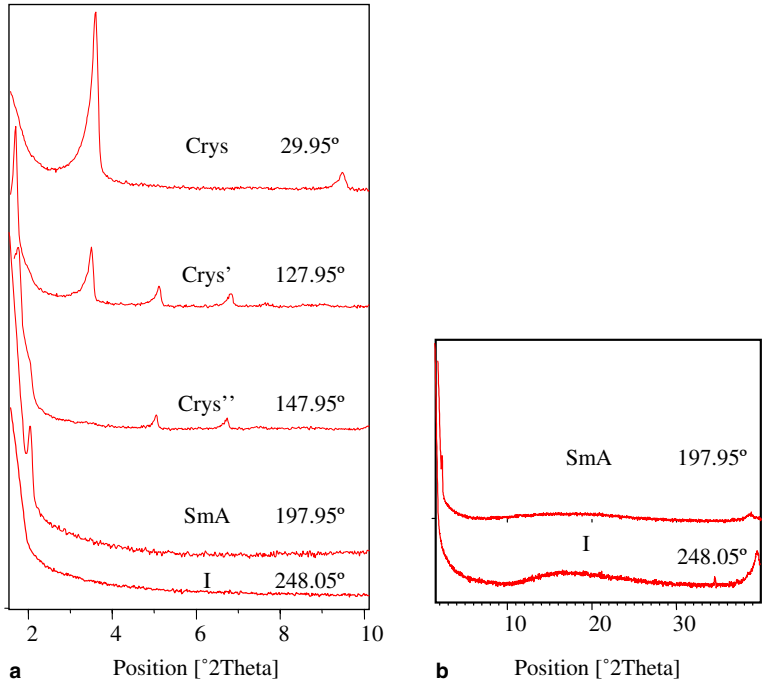

Fig. 8. (a) X-ray diffractograms of *c*-[Pd(η^3-C_3H_5)(pz^{hdp}py)]BF_4 (**15**) at different temperatures in the low-angles region. (b) Full diffractograms for the smectic A mesophase and isotropic liquid of **15**.

15, a molecular length *L* of ca. 34 Å in a fully extended configuration was estimated from the X-ray crystalline structure of **11**. Because the *d*-spacing of the smectic layers (43.34 Å) is larger than *L* (ca. 34 Å), but smaller than 2*L* (ca. 68 Å), we can deduce that the molecules are not arranged in single molecules layers but organised in interdigitated bilayers (Fig. 9). This supramolecular organisation of the mesophase can be related to that of the crystal structure of **11** above described.

On the other hand, complexes **13**–**16** exhibit increased melting temperatures when the length of the alkyl chain is going from 12 to 16 carbon atoms. As deduced from the crystal structures of **11** and **12**, the Pd-containing five-membered ring is essentially planar, in which a partial electron delocalisation suggests certain aromaticity. In addition, the fused pyrazole and pyridine groups are almost coplanar to the Pd-ring as well as the Pd(η^3-C_3H_5) moiety. Therefore, in our complexes, the rigid core, which consists of three aromatic coplanar rings (pyrazole, pyridine and Pd five-membered ring) and a four cycle Pd(η^3-C_3H_5), determines the global geometry of the molecule. Then, the compromise between the rigid planar molecular core and the length of the chains should be reflected in the liquid crystal properties of the complexes.

As it was previously reported, when the contribution of chains prevails the transition temperatures decrease, whereas if contribution of the rigid core prevails temperatures increases [6,34], the latter feature being observed for our complexes. Therefore, it is possible to suggest the presence of core–core interactions to explain the increase of the melting temperatures. Again, from the crystal structures of **11** and **12**, the presence of $\pi\cdots\pi$ interactions was observed, and related interactions could be suggested in the mesophase molecular arrangement.

As conclusion, by comparing the mesogen *c*-[Pd(η^3-C_3H_5)(pz^Rpy)]BF_4 with the non-mesomorphic *c*-[Pd(Cl)$_2$-

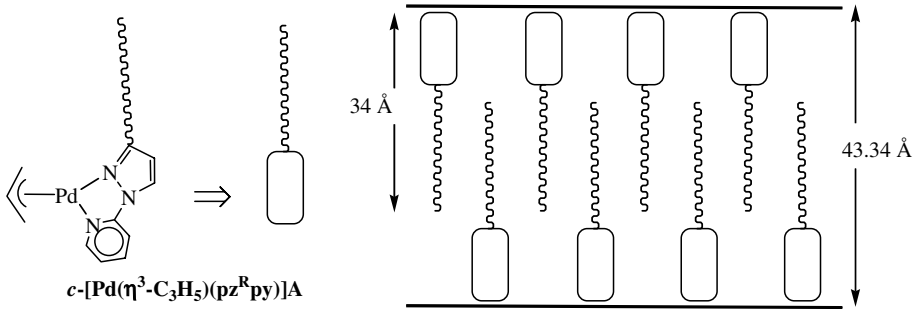

Fig. 9. Proposed molecular arrangement in the smectic A mesophase.

Table 5
Phase properties of *c*-[Pd(η^3-C_3H_5)(pz^{hdp}py)]A (A = BF_4 **15**, PF_6 **17**, CF_3SO_3 **18**)

	Transition	T (°)	ΔH (kJ mol^{-1})
15	Crys → Crys′	79.3	16.2
	Crys′ → Crys″	134.9	11.5
	Crys″ → SmA	169.2	15.0
	SmA → I [a]	244.0	1.7
17	Crys → Crys′	102.4	24.5
	Crys′ → SmA	148.8	14.9
	SmA → I [a]	180.6	0.2
18	Crys → Crys′	59.5	37.3
	Crys′ → SmA	~76.5	
	SmA → I	121.7	0.3

[a] Decomposition.

(pz^Rpy)], it deserves to be noted that the [Pd(η^3-C_3H_5)]$^+$ fragment plays a key role in the improvement of the mesomorphic behaviour. In addition, it is also possible to suggest that the layer-like crystal structure observed for this type of compounds could be related to the lamellar one on the mesophases.

The related compounds containing the same pyrazolylpyridine ligand, pz^{hdp}py, and PF_6^- (**17**) or $CF_3SO_3^-$ (**18**) as counteranions, have also been proved to have liquid crystal behaviour (Fig. 6(c)), showing lower melting and clearing temperatures than the BF_4^- derivative (**15**) (Table 5). Complex **17**, as it was already observed in **15**, exhibits some decomposition at the clearing point. By contrast, complex **18** behaves stable along all the temperature range. Additionally, the improvement of the mesomorphic properties in **18** is evident, displaying the smectic A mesophase at the lowest temperature. By analysing the thermal properties of **15**, **17** and **18**, the influence of the counteranion on the liquid crystal behaviour appears also to be clear. A good molecular packing and strong intermolecular interactions should give rise to high transition temperatures, this feature being observed on the BF_4^- derivative. However the lowest transition temperature observed for **18** agrees with a less efficient packing of the molecules which could be related with the bulkiest and non-symmetrical CF_3-SO_3^- anion.

4. Conclusions

A new series of asymmetric *N*,*N*′-donor ligands of the type 2-[3-(4-alkyloxyphenyl)pyrazol-1-yl]pyridine (pz^Rpy) and their corresponding mononuclear neutral *cis*-dichloropalladium(II) complexes *c*-[PdCl_2(pz^Rpy)] and cationic allylpalladium(II) complexes *c*-[Pd(η^3-C_3H_5)(pz^Rpy)]$^+$ have been prepared and characterised. Neither the ligands nor the $PdCl_2$ derivatives showed mesomorphism, while coordination to the [Pd(η^3-C_3H_5)]$^+$ moiety yielded to metallomesogenic derivatives, confirming the role of the electron delocalisation in the mesomorphism.

The *c*-[Pd(η^3-C_3H_5)(pz^Rpy)]BF_4 complexes with large chains (**13**–**16**) showed crystalline polymorphism and enantiotropic smectic mesomorphism. The lamellar spacing was larger than the estimated molecular length of a single molecule. On this basis, we propose a molecular arrangement in which the molecules in a head-to-tail disposition show interdigitation, giving rise to a semi-bilayered smectic phase.

In addition, the influence of the counteranion on the mesomorphic properties has also been evidenced, the presence of $CF_3SO_3^-$ groups being responsible for the improvement of the mesomorphism.

Acknowledgements

We are grateful to the Dirección General de Investigación/MEC of Spain (Project No. BQU2003-07343) for financial support. We also thank to Comunidad de Madrid for financial support (Project GR/MAT/0511/2004) and the contract to M.C.T. We thank Dr. J. Barberá (Facultad de Ciencias-ICMA, Universidad de Zaragoza-CSIC, Zaragoza, Spain) for your helpful and assessment in the interpretation of the XRD data.

References

[1] M.C. Torralba, M. Cano, J.A. Campo, J.V. Heras, E. Pinilla, M.R. Torres, Inorg. Chem. Commun. 5 (2002) 887.
[2] M.C. Torralba, M. Cano, J.A. Campo, J.V. Heras, E. Pinilla, M.R. Torres, J. Organomet. Chem. 633 (2001) 91.
[3] M.J. Mayoral, M.C. Torralba, M. Cano, J.A. Campo, J.V. Heras, Inorg. Chem. Commun. 6 (2003) 626.
[4] B. Donnio, D.W. Bruce, Struct. Bond. 95 (1999) 193.
[5] M.C. Torralba, M. Cano, J.A. Campo, J.V. Heras, E. Pinilla, M.R. Torres, J. Organomet. Chem. 654 (2002) 150.
[6] M. Ghedini, A. Crispini, Comments Inorg. Chem. 21 (1999) 33.
[7] M. Ghedini, D. Pucci, A. Crispini, I. Aiello, F. Barigelletti, A. Gessi, O. Francescangeli, Appl. Organomet. Chem. 13 (1999) 565.
[8] J. Buey, G.A. Díez, P. Espinet, S. García-Granda, E. Pérez-Carreño, Eur. J. Inorg. Chem. (1998) 1235.
[9] M.J. Baena, J. Buey, P. Espinet, C.E. García-Prieto, J. Organomet. Chem. 690 (2005) 998.
[10] L. Díez, P. Espinet, J.A. Miguel, M.P. Rodríguez-Medina, J. Organomet. Chem. 690 (2005) 261.
[11] F. Neve, M. Ghedini, A. Crispini, Chem. Commun. (1996) 2463.
[12] F. Neve, M. Ghedini, A. Francescangeli, S. Campagna, Liq. Cryst. 24 (1998) 673.
[13] D. Pucci, G. Barberio, A. Crispini, M. Ghedini, O. Francescangeli, Mol. Cryst. Liq. Cryst. 395 (2003) 155.
[14] F. Neve, Adv. Mater. 8 (1996) 277.
[15] M. Ghedini, D. Pucci, J. Organomet. Chem. 395 (1990) 105.
[16] A. El-ghayoury, L. Douce, A. Skoulios, R. Ziessel, Angew. Chem. Int. Ed. 37 (1998) 1255.
[17] K. Ohta, H. Muroki, K.I. Hatada, I. Yamamoto, K. Matsuzaki, Mol. Cryst. Liq. Cryst. 130 (1985) 249.
[18] G.M. Sheldrick, SHELXL97, Program for Refinement of Crystal Structure, University of Göttingen, Germany, 1997.
[19] J.A. Campo, M. Cano, J.V. Heras, M.C. Lagunas, J. Perles, E. Pinilla, M.R. Torres, Helv. Chim. Acta 85 (2002) 1079.
[20] M.L. Gallego, M. Cano, J.A. Campo, J.V. Heras, E. Pinilla, M.R. Torres, P. Cornago, R.M. Claramunt, Eur. J. Inorg. Chem. (2005) 4370.
[21] F. Gómez-de la Torre, A. de la Hoz, F.A. Jalón, B.R. Manzano, A. Otero, A.M. Rodríguez, M.C. Rodríguez-Pérez, Inorg. Chem. 37 (1998) 6606.
[22] F. Gómez-de la Torre, A. de la Hoz, F.A. Jalón, B.R. Manzano, A.M. Rodríguez, J. Elguero, M. Martínez-Ripoll, Inorg. Chem. 39 (2000) 1152.

[23] J. Elguero, A. Fruchier, A. de la Hoz, F.A. Jalón, B.R. Manzano, A. Otero, F. Gómez-de la Torre, Chem. Ber. 129 (1996) 589.
[24] F.A. Jalón, B.R. Manzano, B. Moreno-Lara, Eur. J. Inorg. Chem. (2005) 100.
[25] M.C. Torralba, M. Cano, S. Gómez, J.A. Campo, J.V. Heras, J. Perles, C. Ruiz-Valero, J. Organomet. Chem. 682 (2003) 26.
[26] M. Cano, J.V. Heras, M.L. Gallego, J. Perles, C. Ruiz-Valero, E. Pinilla, M.R. Torres, Helv. Chim. Acta 86 (2003) 3194.
[27] N. Tsukada, T. Sato, H. Mori, S. Sugawara, C. Kabuto, S. Miyano, Y. Inoue, J. Organomet. Chem. 627 (2001) 121.
[28] C.P. Butts, J. Crosby, G.C. Lloyd-Jones, S.C. Stephen, Chem. Commun. (1999) 1707.
[29] P. Bhattacharyya, A.M.Z. Slawin, M.B. Smith, J. Chem. Soc., Dalton Trans. (1998) 2467.
[30] K. Tsutsumi, S. Ogoshi, S. Nishiguchi, H. Kurosawa, J. Am. Chem. Soc. 120 (1998) 1938.
[31] Y. Go, X. Wang, E.V. Anokhina, A.J. Jacobson, Inorg. Chem. 43 (2004) 5360.
[32] H.-Y. Bie, J.-H. Yu, K. Zhao, J. Lu, L.-M. Duan, J.-Q. Xu, J. Mol. Struct. 741 (2005) 77.
[33] P. Gamez, G.A. van Albada, I. Mutikainen, U. Turpeinen, J. Reedijk, Inorg. Chim. Acta 358 (2005) 1975.
[34] G. Vertogen, W.H. de Jeu, Thermotropic Liquid Crystals. Fundamentals, Springer, Heidelberg, Germany, 1988.